Acta Technologica Agriculturae 2
Nitra, Slovaca Universitas Agriculturae Nitriae, 2023, pp. 99–107

THERMOECONOMIC ANALYSIS OF ORGANIC RANKINE CYCLE FROM NAPIER GRASS BIOMASS

Diki Ismail PERMANA*[1, 2], Dani RUSIRAWAN[2], István FARKAS[3]

[1]Hungarian University of Agriculture and Life Sciences, Szent Istvan Campus, Doctoral School of Mechanical Engineering, Gödöllő, Hungary
[2]Institut Teknologi Nasional Bandung, Faculty of Industrial Technology, Department of Mechanical Engineering, Bandung, Indonesia, danir@itenas.ac.id
[3]Hungarian University of Agriculture and Life Sciences, Szent Istvan Campus, Institute of Technology, Gödöllő, Hungary, Farkas.Istvan@uni-mate.hu
*correspondence: dicky91permana@itenas.ac.id

The organic Rankine cycle (ORC) power plant is derived from a centrifugal chiller air conditioning system as an alternative to a diesel replacement modular power plant due to its low cost compared to ORC's manufacture. Biomass is used as a heat source for the power plant to utilize a vast amount of biomass in Indonesia. Research is performed by designing an ORC with biomass that produces around 200 kWe. Simulation done by Microsoft Excel and Reference Fluid Thermodynamic and Transport Properties Database (Lemmon et al., 2013) add-on from the National Institute of Standard Technology (NIST) is used to simulate operating conditions and performance parameters to find a suitable specification of an HVAC system to be modified as an ORC with biomass fuel. Furthermore, based on input from the simulation result and assumptions, other simulation is performed to define operating conditions and types of working fluids, giving the lowest purchase equipment cost. The operating condition analysis of working fluids shows that R123 and R245fa are suitable to be utilized as a potential working fluid for ORC power plants with biomass fuel.

Keywords: elephant grass; working fluid; performance analysis; simulation; cost analysis

Electricity is one of the essential infrastructures to support country's economic growth. The Government of Indonesia has stated that the electricity ratio target of 99.7% must be achieved by 2025. To achieve the target, electricity transmission must cover all areas of Indonesia, including rural areas, isolated systems, and small islands. According to a projection of growth in electricity demand in Indonesia with the optimistic assumption of economic growth for 10 years with an average of 5.2% per year and moving from the realization of electricity demand in 2019, it will reach 379 TWh or undergo an average growth of 4.57% in 2029 as estimated (PLN, 2020). In that report, the government has set a target for the energy mix of the power plant by the end of 2025 for coal at 54.4%, renewable energy at 23%, oil and gas at 22.2% and 0.4%, respectively (PLN, 2020). Until 2020, a renewable energy power plant installed capacity in Indonesia was 63.3 GW, with the contribution of hydropower plants at 8%, the geothermal power plant at 4%, and other renewable energy resources power plants at 1%. The total share of renewable energy power plants was 11% (Electricity Supply Business Chain, 2022). From existing renewable energy sources, not all of them can be directly converted to electricity but require other systems, namely ORC application.

OCR applications have been widely applied, from various heat sources such as excess geothermal steam (Permana et al., 2021), solar thermal utilization (Permana et al., 2022), industrial waste heat, and biomass, where biomass is derived from organic material such as trees, plants, and agricultural and urban waste. Additionally, short rotation coppice provides solid biomass, while agriculture also provides by-products and residues such as biowaste (Hlinka et al., 2019) used for bioheat, biopower and biodiesel (Kristyadi et al., 2022). Many authors have researched related ORC system that uses agricultural biomass as a heat source. Borsukiewicz-Gozdur et al. (2014) conducted a study about to the ORC fuelled by sawmill biomass, and the results indicate that with the proper working fluid (methylcyclohexane), the highest electricity was obtained for the system with internal regeneration. Cao et al. (2021) conducted a thermoeconomic comparison of waste heat from biomass via an ORC system. The result indicated that the waste utilization for compressor inlet cooling could be used for power generation. However, most studies on ORC systems with heat sources from biomass combustion are combined heat power or cogeneration (Uris et al., 2017; Jang and Lee, 2018; Algieri, 2016) and heating district (Prando et al., 2015; Delmastro et al., 2015). On the other side, Tosun (2015) evaluated a 5 MW hybrid ORC from agricultural biomass heat sources, the result is electricity generation at 60–70% thermal performances by cogeneration. Based on the literature presented, most of the existing studies are centred on the ORC system as the second unit of biomass power generation, so there are still limited studies using a single ORC system with a heat source from biomass. In this study, the type of biomass used is Napier grass. Napier grass was chosen because it is one of the bioenergy that is suitable for cultivation in almost all climates and soil

conditions in Indonesia, with a high heating value (HHV) reaching 16.56–18.11 MJ·kg^{-1} (Said et al., 2019). The objective of this study is to evaluate the thermoeconomic performance of Napier grass as a biomass heat source that will be performed using the ORC analysis.

Material and methods

ORC thermodynamic modelling

Figure 1 shows the scheme of the main ORC, including the evaporator, expander, condenser, and feed pump. The heat source for the ORC power plant is obtained from the biomass direct combustion system in the boiler. The heat from biomass combustion is used to heat the heat transfer fluid (HTF) using pressurized water to a specific temperature. The HTF from the boiler flows to the evaporator carrying heat which will be transferred to the ORC's working fluid. After passing through the HTF evaporator, it is pumped back to the boiler to be heated. This system is called the heating circuit (red cycle). The heat dissipation system uses cooling water pumped into the condenser to extract heat from the working fluid. After passing the condenser, the cooling water is cooled in the mechanical draft of the cooling tower using ambient air with the help of an exhaust fan. The cooled water collects under the cooling tower and then is pumped with the cooling tower pump back to the condenser. This system is called a cold circuit (blue cycle). The equations in each main component are as follows (Moran et al., 2008):

Process 1–2, expander:

$$\dot{W}_{\exp} = \dot{m}(h_1 - h_2)\eta_{\exp} \tag{1}$$

Process 2–3, condenser:

$$\dot{Q}_{cond} = \dot{m}(h_2 - h_3) \tag{2}$$

Process 3–4, pump:

$$\dot{W}_p = \dot{m}(h_4 - h_3)\eta_{pump} \tag{3}$$

Process 4–1, evaporator:

$$\dot{Q}_{eva} = \dot{m}(h_1 - h_4) \tag{4}$$

Net power output:

$$\dot{W}_{net} = \dot{W}_{\exp} - \dot{W}_{pump} = (h_1 - h_2) - (h_4 - h_3) \tag{5}$$

Thermal efficiency:

$$\eta_{thermal} = \frac{\dot{W}_{net}}{\dot{Q}_{eva}} = \frac{\dot{W}_{\exp} - \dot{W}_{pump}}{\dot{Q}_{eva}} \tag{6}$$

where: $\dot{W}_{\exp}$, $\dot{W}_p$ – the work on expander and pump, respectively; m – mass flow rate (kg·s^{-1}); h – specific enthalpy (kJ·kg^{-1}); $\dot{Q}_{eva}$, $\dot{Q}_{cond}$ – the heat entering and leaving the system

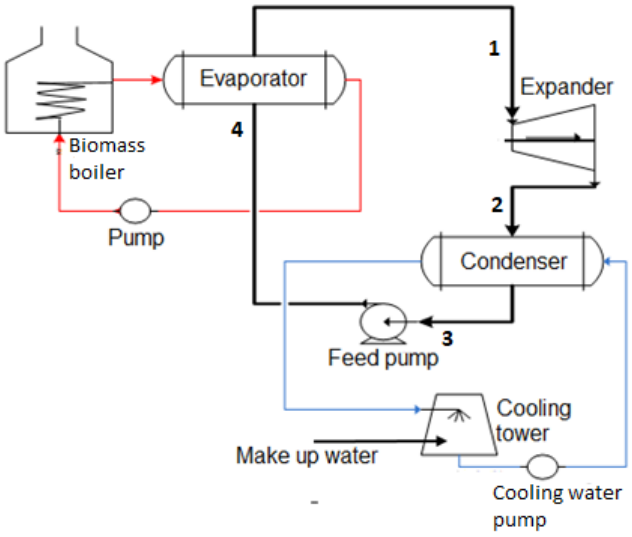


Fig. 1 Design of ORC using biomass heat source

All the equations are valid for an ideal condition where all losses are ignored. In actual conditions, many losses occur, including an increasing entropy in the compression and expansion process. In this study, the isentropic efficiency for the expander (η_{exp}) is set up at 85% and for the pump (η_{pump}) at 90%. The main ORC components such as the expander, condenser, pump, and evaporator are calculated in more detail to determine the cycle performance obtained and will affect the thermoeconomic result. To calculate the mass flow rate of the working fluid through the expander when operating, the Stodola Steam Cone rule is shown by Eq. (7):

$$\dot{m} = \mu_T \cdot C_T \sqrt{p_{in} \cdot \rho_{in}} \sqrt{1 - \frac{1}{\pi}} \tag{7}$$

where: $\pi = p_{in}/p_{out}$ – the pressure ratio; μ_T – the expander nozzle position; C_T – the expander constant value (1.41, 1.65, 1.90, 2.14, and 2.38) derived from the centrifugal chiller compressor with capacities of 300, 350, 400, 450, and 500 TR, respectively

The amount of heat that occurs in the heat exchanger is calculated by the *LMTD* method using Eqs. (8)–(14):

$$Q = U\,A\,LMTD \tag{8}$$

where: Q – the amount of heat needed by the evaporator and condenser (kJ); U – heat transfer coefficient in the evaporator; A – the cross-sectional area (m^2); *LMTD* – log mean temperature difference (°C)

$$LMTD = \frac{(Th_{in} - Tc_{out}) - (Th_{out} - Tc_{in})}{\ln \frac{(Th_{in} - Tc_{out})}{(Th_{out} - Tc_{in})}} \tag{9}$$

$$U = \frac{1}{\frac{2}{\alpha_e} + R_{fo} + \frac{\Delta xw}{k_w} + R_{ft}\frac{\alpha_i}{\alpha_e}} \tag{10}$$

$$\alpha_e = 0.36\frac{\lambda}{D_e}\mathrm{Re}^{0.55}\,\mathrm{Pr}^{1/3} \quad (11)$$

$$\alpha_i = C_{if}\frac{\lambda}{D_i}\mathrm{Re}^{0.8}\,\mathrm{Pr}^{1/3} \quad (12)$$

$$\mathrm{Re} = \frac{4\dot{m}_{wf} n_p}{\pi\mu D_i n_t} \quad (13)$$

$$P_r = \frac{c_p\mu}{k} \quad (14)$$

The *LMTD* can be evaluated using Eq. (9), where Th_{in} and Th_{out} is the hot temperature of the fluid that enters and leaves the heat exchanger from biomass heat source (°C), respectively, Tc_{in} and Tc_{out} and is the cold temperature of the fluid that enters and leaves the heat exchanger (°C). U is the total of heat transfer coefficient in the heat exchanger that can be calculated using Eq. (10). α_e and α_i is heat transfer coefficient from the shell side and tube side shown by Eqs. (11–12), respectively. C_{if} is the constant of internal helical fin tube with a value of 0.06–0.061 and with a diameter around 1.9–2.54 cm, respectively. Reynold number (R_e) and Prandtl number (*Pr*) is shown by Eqs. (13) and (14), where: $\dot{m}_{wf}$, μ, D_i, C_p, k are the mass flow rate of working fluid (m·s^{-1}), dynamic viscosity (N·s^{-1}·m^{-2}), inlet diameter of tube (m), specific heat (J·kg^{-1}·K^{-1}), and thermal conductivity (W·m^{-1}·K^{-1}), respectively. Then, Eq. (15) was used to calculate the in the $\dot{m}_{bio}$ biomass boiler.

$$\dot{m}_{bio} = \frac{Q_{evap}}{\eta_{global}\, LHV_{bio}} \quad (15)$$

where: $\dot{m}_{bio}$ – the mass flow rate in the boiler (kg·s^{-1}); Q_{evap} – the heat of evaporator (kW); η_{global} – the global efficiency of the boiler (%); LHV_{bio} – the low heating value of biomass (kJ)

Thermoeconomic analysis of organic Rankine cycle generation

In a new or existing power plant system, the optimization process is used to find the system's operating conditions that can produce the highest thermal efficiency. However, it is also necessary to study the investment costs incurred compared to the final result to determine the feasibility of investing, better known as thermoeconomic analysis. In this study, the analysis is limited to the study of investment costs or purchase equipment costs (PEC) for several components of the ORC power plant using the following equations (Bejan et al., 1996):

For feed pump:

$$PEC_{FP} = 900\left(\frac{W_{FP}}{300}\right)^{0.25} \quad (16)$$

Cooling tower:

$$PEC_{CTP} = 500\left(\frac{W_{CTP}}{300}\right)^{0.25} \quad (17)$$

HTF pump:

$$PEC_{HTFP} = 500\left(\frac{W_{HTFP}}{300}\right)^{0.25} \quad (18)$$

where: W_{FP} – the work by feed pump (kWe); W_{CTP} – the work by cooling tower pump (kWe); W_{HTF} – the work by HTF pump (kWe). Therefore, Eq. (19) is the cooling tower investment cost (PEC_{CT}) according to Peters and Timmerhaus (1991):

$$PEC_{CT} = X_1\dot{m}_{cw}^{x_2} 10^{x_3 AR + x_4 A + x_5 R + x_6} \quad (19)$$

where: $\dot{m}_{cw}$ – the mass flow of cooling water (kg·s^{-1}); A – the difference of $T_{cw\text{-}in}$ and $T_{wb\text{-}ambient}$; while R – the difference of $T_{cw\text{-}out}$ and $T_{cw\text{-}in}$. The main component of the ORC power plant consists of the evaporator, condenser, and expander. The investment costs for these three components will be assumed to be one component with information about the investment costs from the catalogue. To find out the current price, the present value formula is used according to Eq. (20), with the assumption that the annual interest rate (i) is 6%, and the past value is the price of centrifugal chiller in 2012:

$$present\ value = past\ value\,(1 + i)^n \quad (20)$$

According to Tereshchenko (2016), investment costs for the heat boiler for biomass-fired ORC generation applications represent 600–800 USD·kWe^{-1}.

Working fluids selection and parameters assumption

The main difference between the ORC and the conventional steam Rankine cycle is the working fluid used in each cycle. Water is used as a working fluid in the conventional steam Rankine cycle, while there are many different working fluids that can be used in the ORC. The thermo-physical, safety, and environmental properties vary from one working fluid to another. The choice of suitable working fluid is an essential key in the cycle efficiency evaluation, net work out, etc. The choice of working fluid has been widely studied in scientific journals, both theoretically, simulated, and in practice, but the optimal selection of working fluid is based on the characteristics of the heat source.

Table 1 shows the refrigerant chosen as the working fluid for the ORC analysis. It can be seen that the two selected working fluids have both critical temperature ($T_{critical}$) and critical pressure ($P_{critical}$) that works in the residual heat

Table 1 Working fluids selection (NIST, 2008)

Working fluids	$T_{critical}$ (°C)	$P_{critical}$ (MPa)	ODP	GWP	Type
R123	183.68	3.662	0.012	76	dry
R245fa	154.01	3.651	0	1030	dry

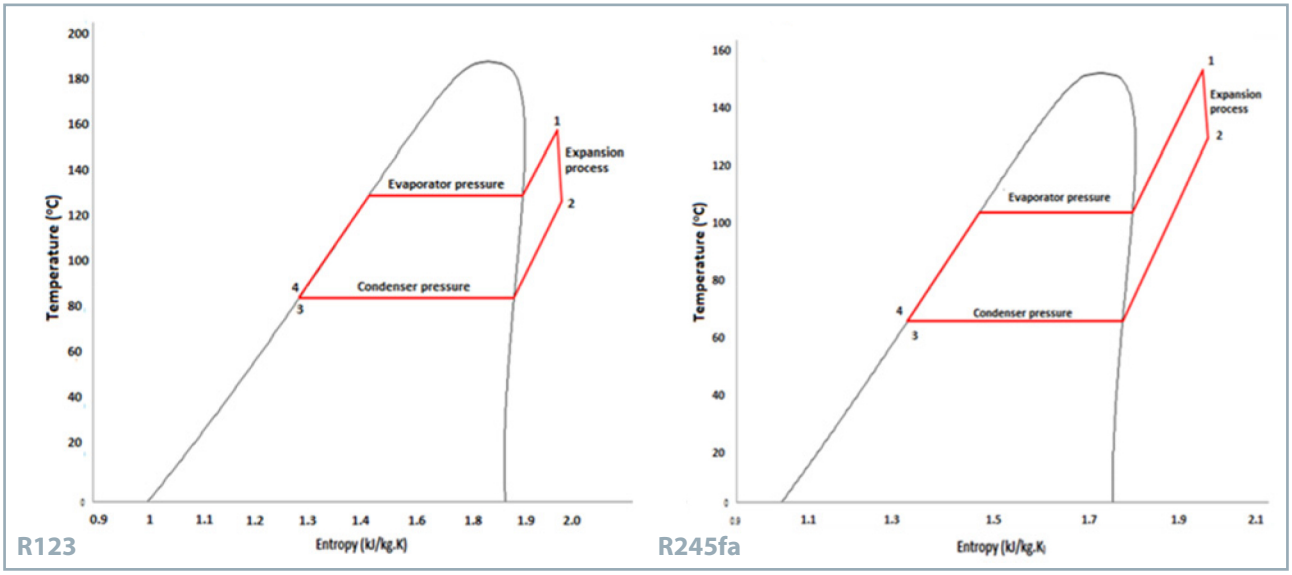


Fig. 2 T-s diagram of working fluids

source temperature and pressure range. Other factors to consider are ozone-depleting potential (ODP) and global warming potential (GWP). These two factors (ODP and GWP) are determined by the heat transfer fluid that can affect the environment in this case in terms of ozone and global warming. For example, the two working fluids (R123 and R245fa) have an ODP of 0, which means the working fluids do not affect the ozone layer. Meanwhile, Fig. 2 shows the T-s diagram of working fluids (R123 and R245fa) in the ORC process cycle.

In this study, most of the main components of the ORC power plant come from the heating, ventilation and air-conditioning (HVAC) system; therefore, the maximum operating parameters of the HVAC system will be assumed as the operating limit of the ORC. The assumptions used are as follows:

1. the maximum temperature and pressure that can be operated by the centrifugal chiller are 160 °C and 1.4 MPa, respectively;
2. $\eta_{exp} = 0.8$, $\eta_{feed\ pump} = 0.7$, $\eta_{generator} = 0.9$;
3. P_{in} and P_{out} of the HTF pump is 0.8 MPa and 1 MPa, respectively;
4. P_{in} and P_{out} of the cooling water pump is 0.15 MPa and 0.3 MPa, respectively;
5. the outlet temperature of cooling water is 29.5 °C;
6. the outlet temperature of the HTF boiler is 170 °C;
7. the efficiency of global biomass heat transfer is 0.85.

Proximity analysis of Napier grass

In the direct combustion process of the biomass boiler, the biomass used is Napier grass (*Pennisetum purpuerum*) with

Table 2 Proximity data and ultimate analysis of Napier grass

Properties	Biomass		
Proximity analysis (wt. %)	**NGS**	**NGL**	**NGT**
Water content	75.27 ±0.21	62.25 ±0.14	74.22 ±0.17
Volatile matter	81.51 ±0.30	79.06 ±0.26	85.17 ±0.21
Ash content	1.75 ±0.01	4.00 ±0.03	6.34 ±0.01
Fixed carbon	16.74 ±0.09	16.94 ±0.04	8.49 ±0.02
HHV (MJ·kg^{-1})	18.11 ±0.10	16.21 ±0.10	16.58 ±0.10
Ultimate analysis (wt. %)			
Carbon (C)	48.61 ±0.80	44.17 ±0.73	45.19 ±0.70
Hydrogen (H)	6.01 ±0.14	5.51 ±0.14	5.93 ±0.15
Nitrogen (N)	0.99 ±0.03	1.01 ±0.03	1.45 ±0.04
Sulphur (S)	0.32 ±0,01	0.27 ±0.01	0.35 ±0.01
Oxygen (O)	44.07 ±0.66	49.04 ±0.74	47.17 ±0.71
O/C (atomic ratio)	0.91	4.00 ±0.03	1.05
O/H (atomic ratio)	0.124	1.11	0.131

Source: Mohammed et al., 2015

Table 3 Performance parameter in the condenser

Condition parameter	Pinch temperature variation (°C)			
	R123		R245fa	
	5	15	5	15
LMTD	19.50	30.26	16.97	26.55
***Q* (kW)**	3264.57	3275.22	3503.63	3538.78
***U* ($W \cdot m^{-2} \cdot K^{-1}$)**	254.95	259.30	548.63	561.31
***A* (m^2)**	656.38	417.37	376.24	237.36

the proximate data and the ultimate analysis for stems (NGS), leaves (NGL), and mixed between stems-leaves (NGT), as shown in Table 2. In this study, the combustion calculation in the biomass boiler uses data from the high heating value (HHV) of the mixed between stems-leaves (NGT) in Table 2, in order to obtain the low heating value (LHV_{dry}) using Eq. (21), where *H* is the fraction of hydrogen (Tariq et al., 1994).

$$LHV_{dry} = HHV_{dry} - 2.442 \times 8.396 \times \frac{H}{100} \quad (21)$$

Results and discussion

This chapter discusses the study results of the energy balance, design condition, and thermoeconomic calculations from the ORC analysis using the equations in the previous chapter and including several literatures to strengthen the results of the analysis.

Results of energy performance

The effect of condensation temperature on the maximum power produced by the expander can be analysed to determine the appropriate capacity of the centrifugal chiller to be converted into an ORC system.

Figure 3 is the characteristic of the change in condensation temperature against the power produced in the ORC system with the expander capacity variations from 350 TR to 550 TR on different working fluids (R123 and R245fa). Figure 3a shows that for the working fluid R123, the condensation temperature which produces the maximum expander circulation is 85 °C. At the same time, the expander power, which produces more than 200 kW of power, is obtained by using a centrifugal chiller capacity of 500 TR. Taking into account the generator and motor losses and the pump's power required, the appropriate expander to produce a net electrical output of 200 kWe is 550 TR. Figure 3b indicates that the condensation temperature that produces the most significant power for the working fluid R245fa is 65 °C. The expander power of more than 200 kW is obtained by using a capacity of 450 TR. By calculating the same losses (generator, motor, and pump), the selected capacity to produce a net electrical output of 200 kWe is 500 TR.

Condenser operation condition

To obtain the operating conditions of the ORC plant that produces a net electrical energy output of around 200 kWe, the operating conditions of the evaporator and condenser must also be considered. This is because both components will determine the energy required by supporting components, e.g., cooling tower fan, pump, and HTF pump. So, the operating conditions that require less energy will result in a more negligible component investment cost. Table 3 shows the performance parameter in the condenser using R123 and R245fa with pinch temperatures at 5 °C and 15 °C. It can be seen that R123 has the highest LTMD value, around 30.26 at 15 °C. However, for *Q* and *A* values, R245fa has the highest value, around 3538 kW and 237.36 m^2, respectively.

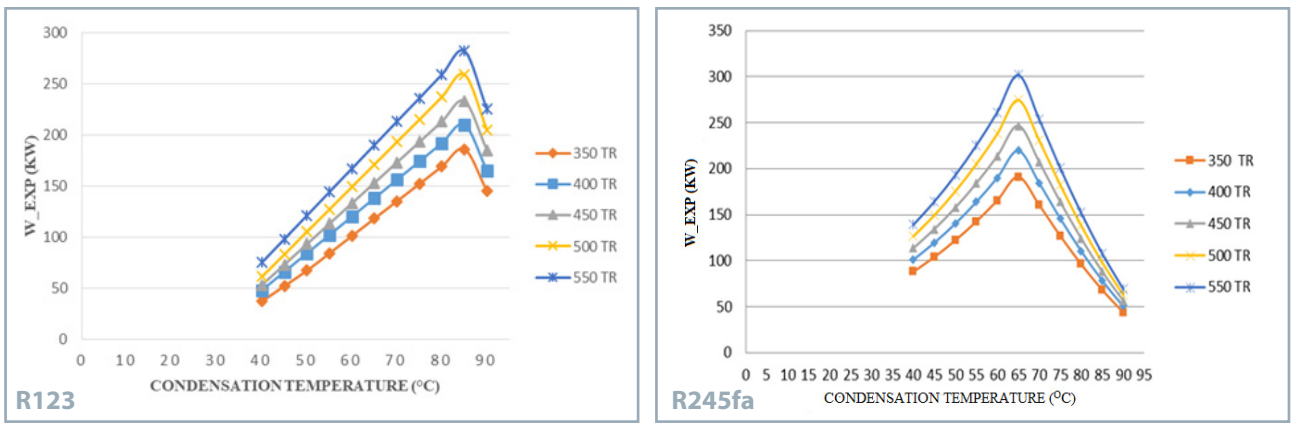


Fig. 3 Condensation temperature vs output work for every variation of the expander capacity from 350 to 550 TR

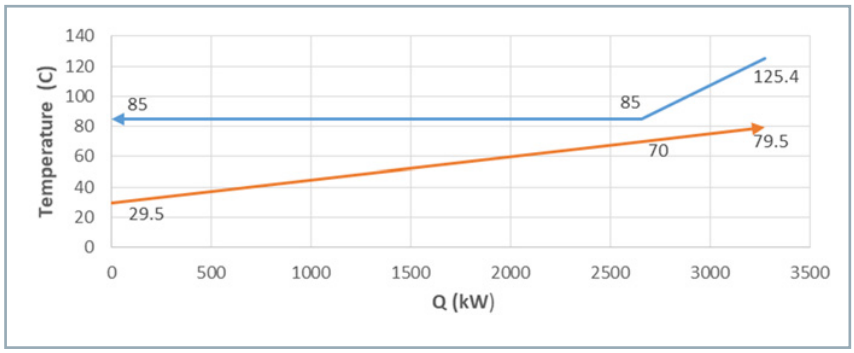


Fig. 4 Temperature profile in the condenser using R123 at the pinch temperature of 15 °C

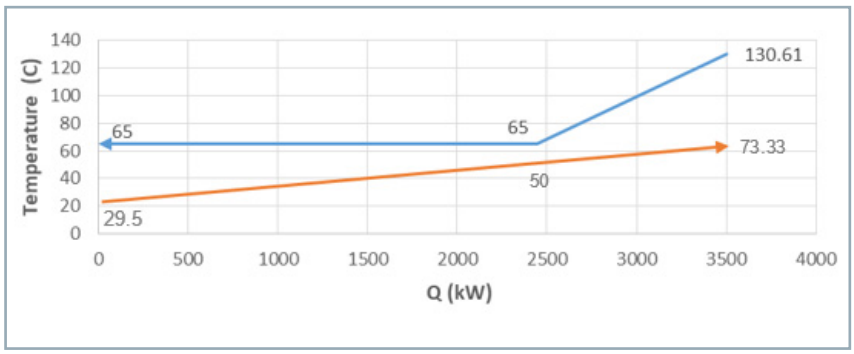


Fig. 5 Temperature profile in the condenser using R245fa at the pinch temperature of 15 °C

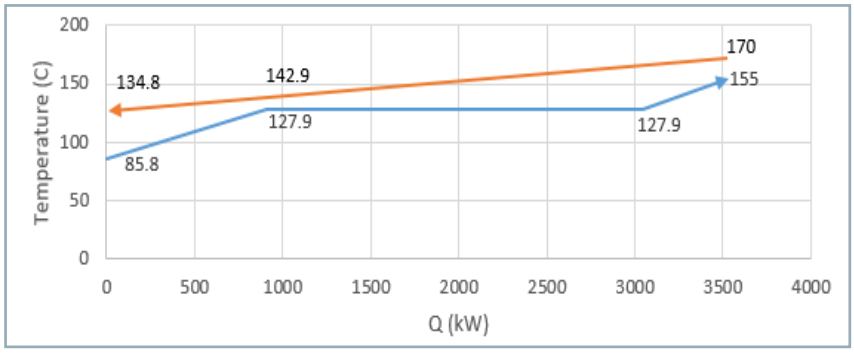


Fig. 6 Temperature profile in the evaporator using R123 at the pinch temperature of 15 °C

In Fig. 4, the R123 enters the condenser in superheated condition at the temperature of 125.4 °C. Due to heat transfer between the working fluid and cooling water, the R123 temperature drops to 85 °C with a mass flow rate of 14.57 kg·s^{-1}, and conversely, the cooling water temperature increases from 29.5 °C to 79.5 °C. The same phenomenon is shown in Fig. 5, where R245fa experiences a significant temperature drop from 130.61 °C to 65 °C. It is due to the two working fluids condensing pressure set inside the condenser must be the same (0.8 MPa), while the condensing temperature properties of the two working fluids are different.

Evaporator operation condition

In the evaporator, the working fluid undergoes heating, evaporating, and superheating processes. At the same time, the HTF on the hot circuit side is maintained in the liquid phase so that the HTF temperature to the evaporator is limited by the water evaporation temperature at 212 °C (2 MPa) and the evaporation exit temperature at 170 °C (0.8 MPa). Table 4 shows the evaluation of the evaporator performance is carried out using the weighted temperature difference (WTD) method with two different pinch temperatures (5 °C and 15 °C) between the inlet temperature of evaporator and expander. It is because the process in the evaporator consists of two types of fluid flow, namely mixed-phase flow and single-phase flow consisting of liquid and vapour.

It can be seen in Table 4 that R245fa has the highest LTMD value of around 36.09, followed by R123 with 29.23 at the same pinch temperature (15 °C). For the Q value at 15 °C, R123 and R245fa have the highest value of around 3752 kW and 3533 kW, respectively. However, for A, the R245fa working fluid with the pinch temperature of 15 °C has the lowest value with 703.08 m^2, followed by the R123 working fluid with 889.78 m^2 at the same pinch temperature (15 °C). Figures 6 and 7 show the temperature profile for R123 and R245 inside the evaporator, respectively.

Table 4 Performance parameter in the evaporator

Condition parameter	Pinch temperature variation (°C)			
	R123		R245fa	
	5	15	5	15
LMTD	17.74	29.23	21.31	36.09
***Q* (kW)**	3523	3533	3752	3752
***U* (W·m^{-2}·K^{-1})**	146.29	135.84	163.81	147.87
***A* (m^2)**	1357.24	889.78	1075	703.08

Table 5 The result of ORC simulation for R123 and R245fa

Working fluids	$\dot{m}_{wf}$ (kg·s^{-1})	$\dot{m}_{HTF}$ (kg·s^{-1})	$\dot{m}_{cw}$ (kg·s^{-1})	$\dot{m}_{air}$ (kg·s^{-1})	T_{CWout} (°C)	Q_{cond} (kW)	Q_{evap} (kW)	W_{exp} (kW)	W_{FP} (kW)	η_{ORC} (%)
R123	18.89	16.56	31.45	72.18	54.80	3329.03	3581.11	269.7	17.60	7.04
R245fa	15.32	11.35	48.16	78.31	47.43	3609.86	3865.75	271.1	15.25	6.62

$\dot{m}_{wf}$ – the mass flow rate of working fluid (kg·s^{-1}); $\dot{m}_{HTF}$ – the mass flow rate of heat transfer fluid (kg·s^{-1}); $\dot{m}_{cw}$ – the mass flow rate of cooling water (kg·s^{-1}); $\dot{m}_{air}$ – the mass flow rate of air (kg·s^{-1}); T_{CWout} – the outlet temperature of cooling water (°C); Q_{cond} – the heat of condenser (kW); Q_{evap} – the heat of evaporator (kW); W_{exp} – the work on expander (kW); W_{FP} – the work on feed pump (kW); η_{ORC} – the efficiency of ORC (%)

Table 6 Total investment cost of the ORC unit

Component	Cost (USD)	
	R123	**R245fa**
ORC unit	159,072.097	143,164.88
Boiler	140,000	140,000
Cooling tower (PEC_{CT})	342,719.03	174,988.26
Feed pump (PEC_{FP})	2480.83	2387
HTF pump (PEC_{HTFP})	871.03	790.60
Cooling tower pump (PEC_{CTP})	912.74	1004.68
Total cost	646,055	462,336
USD·kW^{-1}	3230.28	2311.68

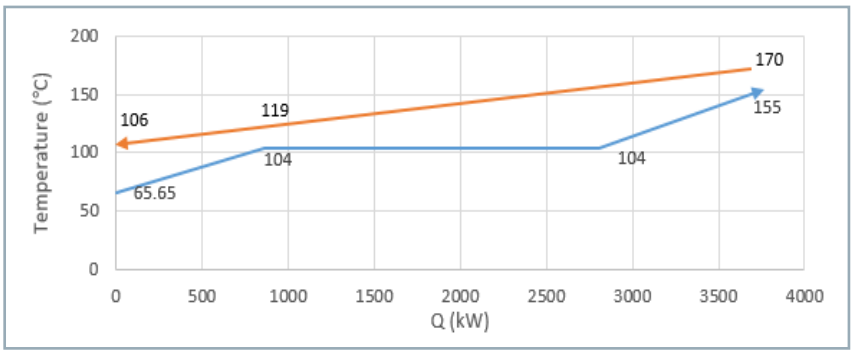


Fig. 7 Temperature profile in the evaporator using R245fa at the pinch temperature of 15 °C

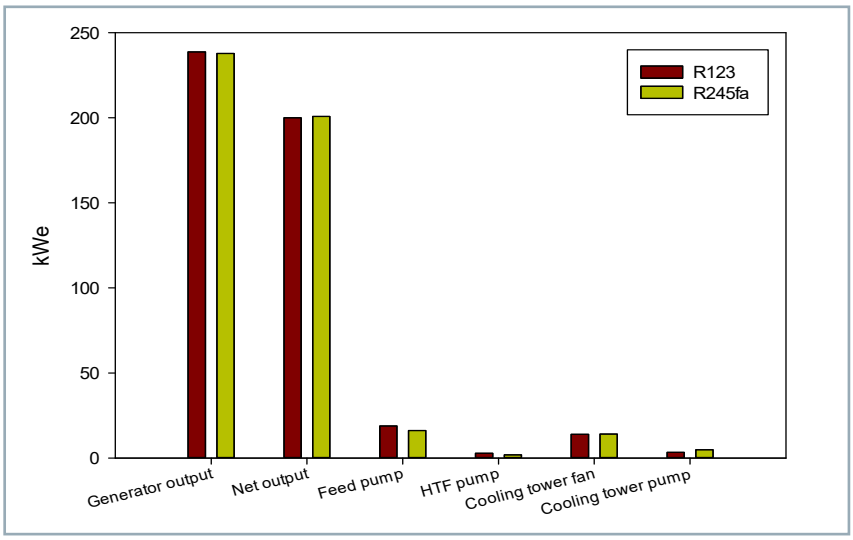


Fig. 8 Electrical consumption of each component

However, in this study, the capacity of the output power generated by the ORC has been determined, which is around 200 kWe. Table 5 shows the result of ORC simulation containing each state of parameters and the amount of thermal efficiency obtained by the two working fluids (R123 and R245fa). We can see the highest Wexp obtained by R245fa with 271.1 kW, followed by R123 with 269.7 kW. As for the ORC performance, ηORC was 7.04% achieved by R123, followed by R245fa with 6.62%.

Electricity consumption and investment cost of ORC

Figure 8 shows that the electrical output of the two working fluids is relatively the same, but the working fluid R123 produces a higher electrical output of 238.78 kWe, followed by R245fa with 237.82 kWe. This trend is followed by components that require electricity, such as feed pumps and HTF pumps, where R123 requires slightly more electricity than the ORC system with the working fluid R245fa. However, for the cooling tower fan and cooling tower pump, R245fa requires more electricity with 14.09 and 4.89 kWe, compared to R123 with 13.86 and 3.33 kWe, respectively.

Table 7 Biomass fuel demand based on working fluid difference

Working fluid	$Q_{biomass}$ (kW)	$\dot{m}_{biomass}$ (kg·s^{-1})	$\dot{m}_{biomass}$ (ton·day^{-1})	$\dot{m}_{biomass}$ (ton·yr^{-1})	Land area (ha)
R123	4213.07	0.25	21.69	7918	226.24
R245fa	4547.9	0.27	23.41	8547	244.22

Based on Table 6, the investment cost of components with R123 requires the most considerable cost between the two types of working fluids. R123 requires an investment cost of ORC power plant components of 3230.28 USD·kW^{-1}, compared to R245fa with 2311.68 USD·kW^{-1}. As operating conditions in the condenser have the greatest effect on the difference in investment costs, that will impact the cooling tower investment costs. This condition occurred because the calculation of the cooling tower investment costs based on the thermoeconomic equations is strongly influenced by the outlet temperature of the cooling water to the cooling tower. The lower the temperature is required, the higher the cost of the cooling tower investment. In contrast to the centrifugal chiller and boiler investment cost calculations, the cooling tower investment costs based on thermoeconomic calculations can be reduced by lowering the cooling water outlet temperature. This can be done by increasing the mass flow rate of cooling water to the condenser.

Biomass fuel demand

According to Table 2, the LHV value per kilogram of Napier grass biomass is 16,779 kJ·kg^{-1}. According to Mohammed et al. (2015), in the best conditions, Napier grass can be harvested four times a year with an average yield of 8.75 dry tons per hectare. Assuming that the availability factor (AF) of ORC power plants per year is 0.85, the demand for Napier grass biomass for ORC power plants with different working fluid (R123, R245fa) for one year of operation can be seen in Table 7.

From the calculations that have been carried out related to performance, component investment costs, and biomass requirements for ORC power plants based on the working fluid (R123, R245fa), it can be seen that there is no one type of working fluid that is genuinely superior to be selected as a single fluid job. Each fluid has its advantages and disadvantages. In terms of ORC efficiency, it can be seen that the working fluid R123 has the highest value of 7.04%, followed by R245fa (6.62%). R123 requires the slightest heat, 3581.11 kW, followed by R245fa (3865.75 kW) for the amount of heat input in the working fluid evaporator. This is directly related to the amount of biomass the ORC plant needs and, finally, the area of land required for planting the Napier grass biomass.

Since the initial objective of this research was to find an ORC power plant with a competitive investment cost compared to other types of power plants, the working fluid R245fa was chosen to be the working fluid for the ORC power plant with a component investment cost of 2311.68 USD·kW^{-1}. The need for a land area for planting the Napier grass biomass of 244.22 ha with 21.69 ton·day^{-1} can be overcome by using unproductive lands such as critical land and abandoned mines. According to Mohammed et al. (2015), Napier grass can be planted to fill vacant land in oil palm plantations, estimated to be 26.63% of the total land. Meanwhile, according to Warmanti (2012), Napier grass can be cultivated on sandy land along the coast by using the correct dose of NPK fertilizer.

Conclusion

The thermodynamic study shows that the main components of the centrifugal chiller air conditioning system can be converted into ORC components by determining the proper operating conditions. The simulation results of the thermal cycle of the ORC with working fluids (R123, R245fa) have shown that the thermal efficiency produced is 7.04% for the working fluid R123 and 6.62% for the working fluid R245fa. Furthermore, when calculating the investment costs of the components with different working fluid, it is found that R245fa has a more significant potential to be used as a working fluid than R123 for ORC power plants with biomass fuels with an electrical output of 200 kWe. The reason is that it can provide operating conditions that result in the cheapest component investment costs of 2311.68 USD·kWe^{-1} compared to R123 with 3230.28 USD·kW^{-1}. As a final result, 244.22 ha of land is required for growing Napier grass biomass, which grows at a rate of 21.69 ton·day^{-1}. This demand can be met by exploiting underutilized lands, such as critical land and abandoned mines.

Acknowledgement

This work was supported by the Stipendium Hungaricum Programme of the Doctoral School of Mechanical Engineering, Hungarian University of Agriculture and Life Sciences, Gödöllő, Hungary and the Department of Mechanical Engineering, Institut Teknologi Nasional Bandung (ITENAS Bandung), Indonesia.

References

ALGIERI, A. 2016. Comparative investigation of the performances of subcritical and transcritical biomass-fired ORC systems for micro-scale CHP applications. In Procedia Computer Science, vol. 83, pp. 855–862. DOI: https://doi.org/10.1016/j.procs.2016.04.176

BEJAN, A. – TSATSARONIS, G. – MORAN, M. 1996. Thermal Design and Optimization. John Wiley & Sons Inc. ISBN 978-0-471-58467-4

CAO, Y. – MIHARDJO, L. W. W. – DAHARI, M. – TLILI, I. 2021. Waste heat from a biomass fueled gas turbine for power generation via an ORC or compressor inlet cooling via an absorption refrigeration cycle: A thermoeconomic comparison. In Applied Thermal Engineering, vol. 182, article no. 116117.
DOI: https://doi.org/10.1016/j.applthermaleng.2020.116117

DELMASTRO, C. – MUTANI, G. – SCHRANZ, L. 2015. Advantages of coupling a woody biomass cogeneration plant with a district heating network for a sustainable built environment: A case study in Luserna San Giovanni (Torino, Italy). In Energy Procedia, vol. 78, pp. 794–799. DOI: https://doi.org/10.1016/j.egypro.2015.11.102

ELECTRICITY SUPPLY BUSSINESS CHAIN. 2022. Diseminasi RUPTL 2021-2030. (In Indonesian: Rencana umum penyediaan tenaga listrik/RUPTL 2021-2030). Available at: https://web.pln.co.id/statics/uploads/2021/10/materi-diseminasi-2021-2030-publik.pdf

BORSUKIEWICZ-GOZDUR, A. – WISNIEWSKI, S. – MOCARSKI, S. – BANKOWSKI, M. 2014. ORC power plant for electricity production from forest and agriculture biomass. In Energy Conversion and Management, vol. 87, pp 1180–1185.
DOI: https://doi.org/10.1016/j.enconman.2014.04.098

HLINKA, P. – KARANDUŠOVSKÁ, I. – MIHINA, Š. 2019. Monitoring of gas production during the biowaste composting. In Acta Technologica Agriculturae, vol. 3, pp. 75–79.
DOI: https://doi.org/10.2478/ata-2019-0014

JANG, Y. – LEE, J. 2018. Optimizations of the organic Rankine cycle-based domestic CHP using biomass fuel. In Energy Conversion and Management vol. 160, pp. 31–47.
DOI: https://doi.org/10.1016/j.enconman.2018.01.025

KRISTYADI, T. – PERMANA, D. I. – SIRODS, M. P. N. – SAEFUDIN, E. – FARKAS, I. 2022. Performance and emission of diesel engine fuelled by commercial bio-diesel fuels in Indonesia. In Acta Technologica Agriculturae, vol. 25, pp. 221–228.
DOI: https://doi.org/10.2478/ata-2022-0032

LEMMON, E. W. – HUBER, M. L. – MCLINDEN, M. O. 2013. NIST Standard Reference Database 23: Reference Fluid Thermodynamic and Transport Properties – REFPROP, Version 9.1. National Institute of Standards and Technology (NIST), Gaithersburg, MD. Available at: https://tsapps.nist.gov/publication/get_pdf.cfm?pub_id=912382

MOHAMMED, I. Y. – ABAKR, Y. A. – KAZI, F. K. – YUSUP, S. – ALDHAREEF, I. – CHIN, S. A. 2015. Comprehensive characterization of Napier grass as a feedstock for thermochemical conversion. In Energies vol. 8, pp. 3403–3417. DOI: https://doi.org/10.3390/en8053403

MORAN, M. J. – SHAPIRO, H. N. – BOETTNER, D. D. – BAILEY, M. B. 2008. Fundamentals of Engineering Thermodynamics. 6th ed. USA: Wiley, 978 pp. ISBN 0470495901.

PERMANA, D. I. – RUSIRAWAN, D. – FARKAS, I. 2022. A bibliometric analysis of the application of solar energy to the organic Rankine cycle. In Heliyon, vol. 8, no. 4, article no. e09220.
DOI: https://doi.org/10.1016/j.heliyon.2022.e09220

PERMANA, D. I. – RUSIRAWAN, D. – FARKAS, I. 2021. Waste heat recovery of Tura geothermal excess steam using organic Rankine cycle. In International Journal of Thermodynamics, vol. 24, no. 4, pp. 32–40. DOI: https://doi.org/10.5541/ijot.906128

PETERS, M. S. – TIMMERHAUS, K. D. 1991. Plant Design and Economics for Chemical Engineers. Mc Graw-Hill Education (ISE Editions), 992 pp. ISBN 978-0071008716.

PLN. 2020. Electricity planning projection through RUPTL. Available at: https://gatrik.esdm.go.id/assets/uploads/download_index/files/38622-ruptl-pln-2021-2030.pdf (In Indonesian: Proyeksi perencanaan ketenagalistrikan melalui RUPTL)

PRANDO, D. – RENZI, M. – GASPARELLA, A. – BARATIERI, M. 2015. Monitoring of the energy performance of a district heating CHP plant based on biomass boiler and ORC generator. In Applied Thermal Engineering, vol. 79, pp. 98–107.
DOI: https://doi.org/10.1016/j.applthermaleng.2014.12.063

SAID, M. S. M. – GHANI, W. A. W. A. K. – BOON, T. H. – HUSSAIN, S. A. – SUM NG, D. K. 2019. Thermochemical conversion of Napier grass for production of renewable syngas. In Processes, vol. 7, no. 10, article no. 705. DOI: https://doi.org/10.3390/pr7100705

TARIQ, A. S. – REUPKE, P. – SARWAR, G. 1994. Biomass Combustion Systems. A guide for monitoring and efficient operation. Natural Resources Institute, Chatham, UK.

TERESHCHENKO, T. 2016. Energy planning of future district heating systems with various energy resources. Doctoral thesis, NTNU, Norway.

TOSUN, Y. I. 2015. 5MW hybrid power generation with agriculture and forestry biomass waste co-incineration in stoker and subsequent solar panel (CSP) ORC station. In 2015 International Conference on Renewable Energy Research and Applications (ICRERA), Palermo, Italy, 2015, pp. 583–589.
DOI: https://doi.org/10.1109/ICRERA.2015.7418481

URIS, M. – LINARES, J. I. – ARENAS, E. 2017. Feasibility assessment of an Organic Rankine Cycle (ORC) cogeneration plant (CHP/CCHP) fueled by biomass for a district network in mainland Spain. In Energy, vol. 133, pp. 969–985.
DOI: https://doi.org/10.1016/j.energy.2017.05.160

WARMANTI, M. 2012. Mass weight and heat value of elephant grass at various doses of NPK fertilizer on beach sand. In Jurnal Argrisains, vol. 3, no. 4, pp. 53–62. Available at: http://ejurnal.mercubuana-yogya.ac.id/index.php/Agrisains/article/view/37 (In Indonesian: Bobot massa dan nilai panas rumput gajah pada berbagai dosisi pupuk NPK di lahan pasir pantai, vol. 3(4), pp. 53-62)